

1. Supplementary Text

Statistical tests, significance levels and sample sizes

Distributions (Figs. 2a, g, h, 4C, S4, S7) were compared using the Kolmogorov-Smirnov test. Means were compared using rank-sum test. The statistical significance of the proportion of significant events out of the total number of candidate events was determined as the binomial probability of observing the calculated number of significant events (as successes) from the total number of candidate events (as independent trials), with 0.025 being the probability of success in any given trial. The highest proportion of significant events that was still at chance level varied according to the total number of spiking events (see dotted line in Fig. 2b). Comparisons between proportions were done using the Z-test for two proportions. The median number of cells participating in the preplay events was five in the Contig condition and six in the De novo condition.

Main parameters for the sleep/rest and run sessions

1. De novo pre-run sleep/rest. Mean duration: 53.5 min/session; 55, 53, 79, and 27 min in the 4 mice).
2. De novo run session. Mean duration 49.2 min; 55, 44, 37, 61 min in the 4 mice.
3. The averages of the running speed in the novel track for the four mice were 8.98 ± 0.097 , 9.16 ± 0.044 , 9.15 ± 0.03 , and 9.17 ± 0.048 cm/s, respectively.
4. Contig condition, Fam session: 31, 15, 60, and 26 min for mice 1 through 4, respectively.

5. For all mice, the Fam-Rest session represented 56-76% of the duration of the Fam session (76%, 63%, 56%, and 60% for mice 1 through 4, respectively).
6. Contig session: 34, 42, 34, and 36 min for mice 1 through 4, respectively.
7. For mice 1 through 3, the average running speed in the novel arm was lower than in the familiar arm during Contig-Run (9.6 ± 0.05 vs. 12.1 ± 0.15 cm/s for mouse 1, $p < 10^{-80}$, t-test; 11 ± 0.08 vs. 11.7 ± 0.08 cm/s for mouse 2, $p < 10^{-7}$; 11.7 ± 0.07 vs. 12.5 ± 0.08 cm/s for mouse 3, $p < 10^{-12}$), while the opposite was true for mouse 4 (10.8 ± 0.07 vs. 9.2 ± 0.07 cm/s, $p < 10^{-50}$).

Additional controls for preplay in the Contig condition

1. In order to directly compare preplay and combined forward-reverse replay events¹, we combined forward and reverse half-templates of the familiar track to construct four synthetic unidirectional “combined templates” of the familiar track running from one end of the familiar track to the other. Two of these templates ran from the free end of the familiar track to the junctional end of the novel arm (direction 1), while the other two ran in the opposite direction (direction 2). For instance, considering the two original halves of the track to be A1 and A2 in direction 1 and B1 and B2 in direction 2, the combined synthetic templates were: A1+rB1 and rB2+A2 in direction 1, and B1+rA1 and rA2+B2 in direction 2, where r denotes reverse order of the corresponding half-track sequence. We used these combined templates as control replay for the detected preplay events. We chose the midpoint of the familiar track as the switch point between the forward- and reverse-going sequences based on previous reports² that switches in the spatial reference frame controlling place cell firing mostly occurred at the midpoint of the linear track. We found that 84.4% of the spiking events that were correlated with the novel arm template (preplay events) did not correlate with the combined forward/reverse synthetic templates in any direction. In addition, of the remaining spiking events that correlated with both the novel and the combined templates, 8.9% were more correlated with the novel arm template than with the combined templates. These results indicate that the preplay phenomenon is not a simple combination of forward and reverse replay of a recent familiar experience.

2. Upon barrier removal, some of the place cell activity at the junctional end of the familiar track might spread into the junctional end of the novel arm. This might raise the possibility that these cells might fire in the same order on the novel arm as on the familiar track and thus the preplay events might potentially represent replays of the junctional end of the familiar track. We constructed new novel arm templates in which place cells with fields at the junctional end of the novel arm expressed during Contig-Run and fields at the junctional end of the familiar track during Fam-Run were eliminated from the novel arm templates. These were cells 9, 10, and 11 from Fig. 1A,c, cell 13 from Fig. 1B,c, and cells 3 and 4 from Fig. 1E, c. The familiar track templates were kept unaltered. We then re-ran the correlation calculations using these new templates and found that the proportion of events that significantly correlated with the novel arm but not with the familiar track has dropped only 18%. Thus, the overwhelming majority of the preplay events are not depending on the place cells firing at or near the junction between the 2 arms.

3. We have constructed an additional set of templates, the familiar arm templates, from place cell activity on the familiar arm during Contig-Run. For each preplay event we calculated its correlation with these familiar arm templates. We found that 71.4% of the detected preplay events were not correlated with any of the familiar arm templates, indicating they were true preplay events of the novel arm.

4. We used synthetic templates made from half of the familiar track contiguous with half of the novel track (i.e., around the location of the barrier) to test whether the preplay sequences simply reflect periodic “extensions” of the familiar track representation. Only 2.7% of all the spiking events occurring during Fam-Rest were significantly correlated with these templates at $p < 0.025$ significance level. This proportion of events is not statistically significant ($p > 0.05$, binomial probability test).

Possible reasons for lack of preplay detection in previous studies

1. We have applied the pair-wise temporal bias analysis^{3,4} to test the detection of preplay in animals that had no prior experience on linear tracks as well as during Contig condition. Cross-correlograms were constructed for all cell-pairs separately during run on novel tracks and during sleep or rest periods before the run sessions (± 200 ms around zero, minimum 200 counts/correlogram). Temporal bias was calculated as the difference between the number of counts in the -200 to 0 ms portion of the correlogram and the number of counts in the 0 to 200 ms, normalized by total number of counts of the correlogram⁴, for all cells pairs and both sleep/rest and run sessions. The correlations between the temporal bias during run and the temporal bias during pre-run sleep/rest session averaged across all animals was -0.09, $p=0.62$ for the 4 De novo sessions and -0.03, $p=0.69$ for the 3 Contig sessions ($r=-0.06$, $p=0.51$ for all 7 sessions combined). This indicates that the temporal bias method does not detect preplay on average cross-correlations from 4 mice, consistent with the previous studies^{3,4}. The pair-wise correlation method is not as sensitive as the direct sequences comparison method and can miss preplay events which can be as few as several percents of the total spiking events and can reflect place sequences both in forward and reverse temporal order.
2. In a previous study⁵, the detection of preplay by sequence analysis could have been hampered by the use of a relatively low number and density of place cells (i.e., 8.5 vs. 14 cells/template in our study and 3.5 vs. 9.1 cells/meter of track in our study) and total spiking events (one order of magnitude less than in our study) and/or by the instability/remapping in the run session of some of the cells active during pre-run sleep⁵.

Supplementary data by figures

Figure 2a. Preplay novel arm: Data, $n = 526$ events. Significant, $n = 75$ events.

Figure 2b. Preplay novel arm template (top left panel): 14.2% significant events, 7.03% forward and 7.67% reverse preplay. Remotely initiated significant events: 40.6% of all significant preplay events.

Figure 2d. Proportion of significant events. Total, junction end = 0.81; opposite end = 0.19. Normalized, junction end = 0.15; opposite end = 0.085, $p < 0.035$, Z-test for two proportions.

Figure 2e. Stability of spatial map. Familiar track, data vs. shuffle: 0.66 ± 0.03 versus 0.22 ± 0.016 , $p < 10^{-15}$, rank sum test. Novel arm, data vs. shuffle: 0.62 ± 0.05 versus 0.21 ± 0.03 , $p < 10^{-5}$, rank sum test.

Figure 2g. Expressed out of all spiking events, 4.4% were pure preplay events ($p < 0.000035$, binomial probability test), 13.9% were pure replay events ($p < 10^{-71}$), and 1.5% were preplay/replay events ($p > 0.05$).

Figure 2h. The correlation values (R) are, in order: -0.29, -0.2, -0.14, 0.0, 0.05, 0.2. No correlation had a significance level (P) below 0.05.

Figure 3. The lines fitted to the shuffled data had significantly lower slope ($p < 10^{-41}$, both shuffles), spatial extent ($p < 10^{-70}$, both shuffles), and score ($p < 10^{-5}$, time-bin shuffle) than the lines fitted to the original data, indicating that the Bayesian decoding reconstructs real trajectories that are not simply noise. Shuffle analysis. Original data versus time-bin shuffles: line slope 557 ± 22 vs. 377 ± 0.9 cm/s ($p < 10^{-41}$, Kolmogorov-Smirnov test); spatial extent 38 ± 1.2 vs. 25 ± 0.05 cm ($p < 10^{-70}$, Kolmogorov-Smirnov test); score 0.13 ± 0.002 vs. 0.12 ± 0.0001 ($p < 10^{-5}$, Kolmogorov-Smirnov test).

Original data versus cell-identity shuffles: line slope 557 ± 22 vs. 270 ± 1.7 cm/s ($p < 10^{-87}$, Kolmogorov-Smirnov test); spatial extent 38 ± 1.2 vs. 17 ± 0.09 cm ($p < 10^{-129}$, Kolmogorov-Smirnov test); score – not significantly higher.

Significant novel arm trajectories: 71/89 (79.78%); significant familiar arm trajectories: 325/349 (93.12%); joint novel arm and familiar track trajectories: 106. Absolute rank order correlations between spiking events and novel arm template for novel arm trajectories: 0.75 ± 0.02 . Absolute rank order correlations between spiking events and familiar track template for novel arm trajectories: 0.59 ± 0.03 .

Figure 4B. Preplay novel track: Data, $n = 4316$ events. Significant, $n = 697$ events (16.15%). All individual animals display a significant number of preplay events: Mouse 1, 544/3241 (16.7%); Mouse 2, 14/112 (12.5%); Mouse 3, 73/491 (14.8%); and Mouse 4, 66/472 (13.9%).

Figure 4D. Stability of spatial map. Novel track, data vs. shuffle: 0.42 ± 0.003 versus 0.22 ± 0.04 , $p < 10^{-4}$, rank sum test.

Supplementary figure 4. Number of significant/total events per animal: Mouse 1, 44/226 (19.47%); Mouse 2, 8/34 (23.53%); and Mouse 3, 23/266 (8.65%).

2. Tables 1-3

Breakdown of total number of cells for each animal by activity

Table 1. Both directions

Mouse#	Familiar track and novel arm	Familiar track only	Novel arm only	Familiar track or novel arm	Rest only (silent cells)	Inter-neurons	All cells
1	8	5	4	17	9	1	27
2	8	4	1	13	11	1	25
3	9	4	2	15	6	2	23
4	5	0	0	5	4	3	12
Total	30	13	7	50	30	7	87

Table 2. Direction 1 (familiar track to novel arm)

Mouse#	Familiar track and novel arm	Familiar track only	Novel arm only	Familiar track or novel arm	Rest only (silent cells)
1	5	7	4	16	10
2	5	5	1	11	13
3	7	3	4	14	7
4	1	1	3	5	4
Total	18	16	12	46	34

Table 3. Direction 2 (novel arm to familiar track)

Mouse#	Familiar track and novel arm	Familiar track only	Novel arm only	Familiar track or novel arm	Rest only (silent cells)
1	7	5	4	16	10
2	8	4	1	13	11
3	4	9	2	15	6
4	4	1	0	5	4
Total	23	19	7	49	31

4. Reference List

1. Davidson,T.J., Kloosterman,F. & Wilson,M.A. Hippocampal replay of extended experience. *Neuron* **63**, 497-507 (2009).
2. Redish,A.D., Rosenzweig,E.S., Bohanick,J.D., McNaughton,B.L. & Barnes,C.A. Dynamics of hippocampal ensemble activity realignment: time versus space. *J. Neurosci.* **20**, 9298-9309 (2000).
3. Skaggs,W.E. & McNaughton,B.L. Replay of neuronal firing sequences in rat hippocampus during sleep following spatial experience. *Science* **271**, 1870-1873 (1996).
4. Gerrard,J.L., Burke,S.N., McNaughton,B.L. & Barnes,C.A. Sequence reactivation in the hippocampus is impaired in aged rats. *J. Neurosci.* **28**, 7883-7890 (2008).
5. Lee,A.K. & Wilson,M.A. Memory of sequential experience in the hippocampus during slow wave sleep. *Neuron* **36**, 1183-1194 (2002).

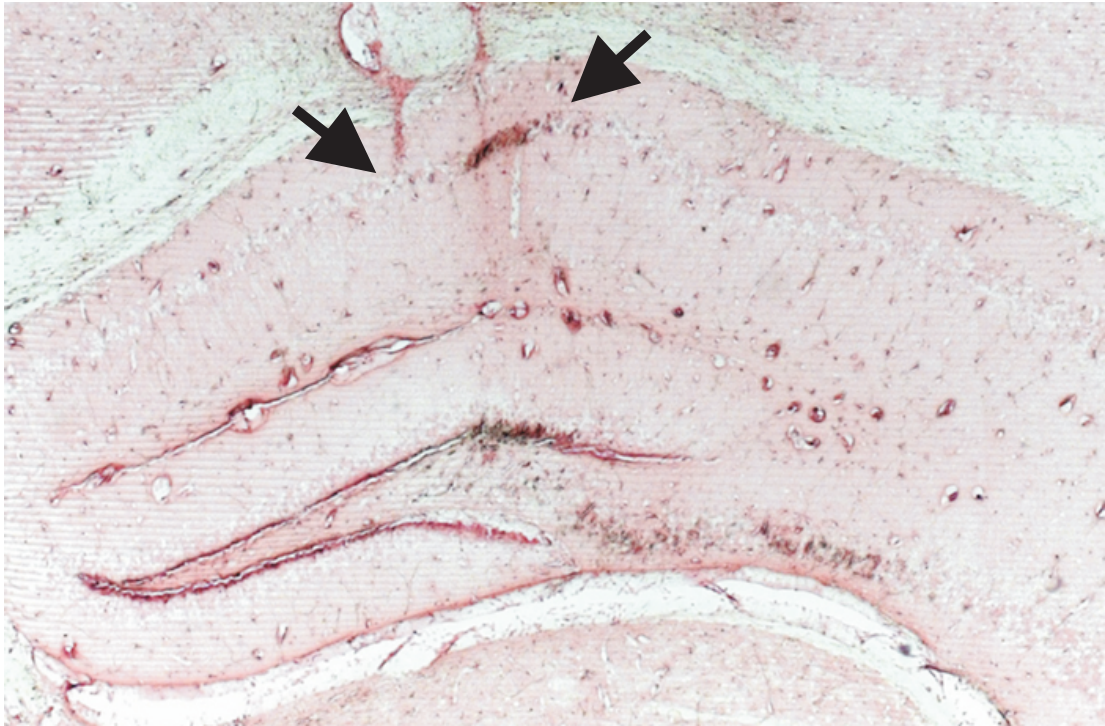


Figure S1 Location of electrodes recording from the CA1 area of the hippocampus in Mouse 3. Arrows mark the extent of recorded CA1 area in this animal. All other animals have a similar area of recording from the CA1 subfield of the hippocampus. Staining: Nuclear fast red.

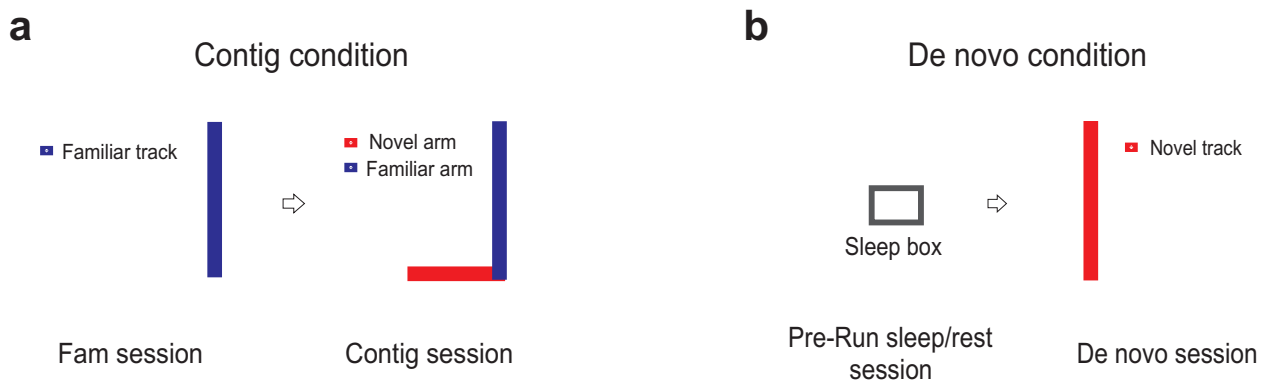


Figure S2 Experimental design a, Experimental apparatus for Contig condition. Left, a linear track (blue) to which the mice were familiarized. Right, an L-shaped track consisting of the familiar arm (blue) and a contiguous novel arm (red). After the mice were familiarized to the linear track, the barrier at one of the two ends was removed so that the mice could explore the entire L-shaped track freely. **b**, Experimental apparatus for the De novo condition. Left, sleep box in which mice were kept prior to being exposed to running on a linear track for the first time. Right, the novel track (red) on which mice had the first run session on a linear track (de novo run session).

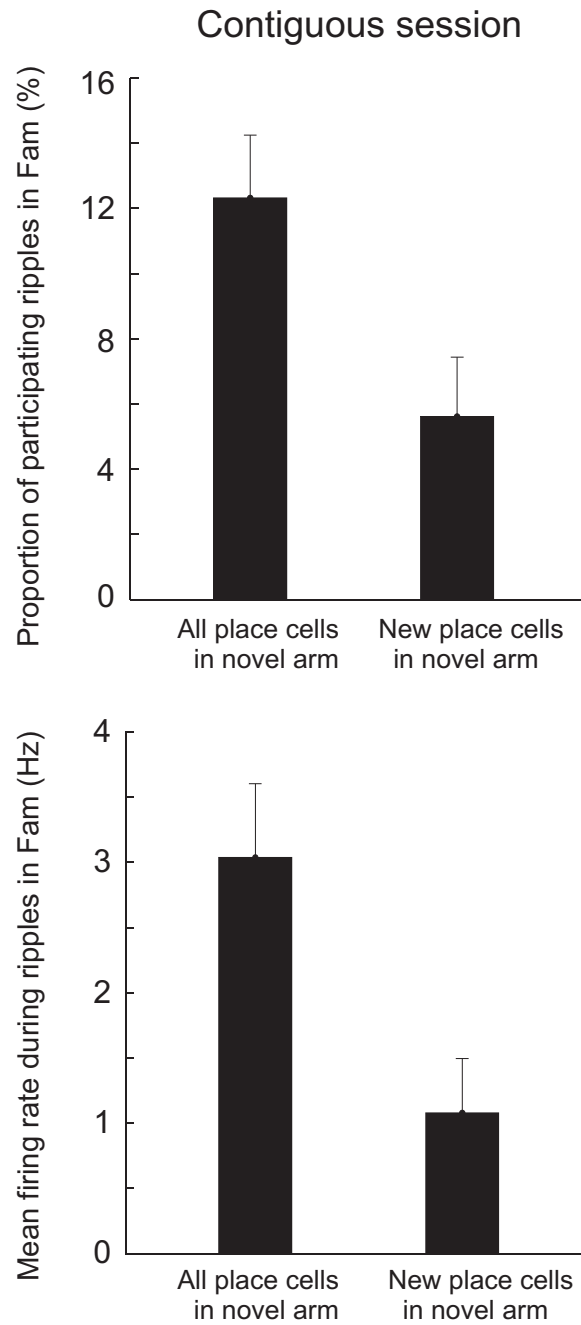


Figure S3 Activity of place cells from the Contig-Run session during Fam-Rest ripple epochs. Proportion of ripples in the preceding familiar track session (Fam) during which place cells active on the novel arm fired (top), and their average firing rates during these ripple epochs (bottom).

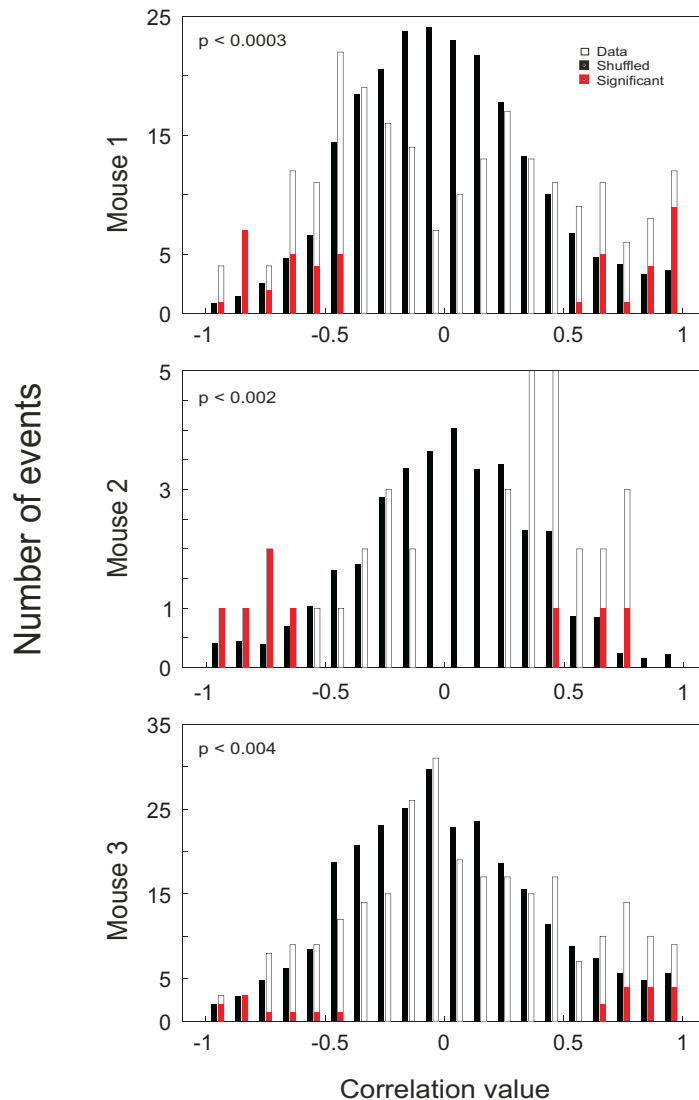


Figure S4 Quantification of the preplay phenomenon in individual mice in the Contig condition. Distribution of spiking events across rank-order correlation with the place cell sequence template of the novel arm for individual animals. The top panel corresponds to examples shown in Fig. 1A-B (Mouse 1), the middle to Fig. 1C-D (Mouse 2), and the bottom to Fig. 1E (Mouse 3). Open bars: spiking events vs. the original (unshuffled) template. Filled bars: spiking events vs. 200 shuffled templates. In order to obtain this distribution, the correlation value of each event vs. each randomly shuffled template was determined and the values from the 200 shuffled templates were scaled down 200 times. Red bars: distribution of significant preplay events (see the text for

the definition of significance). P-values refer to results from the Kolmogorov-Smirnov test. The proportions of significant events out of the total number of spiking events were significant in each animal: $p < 10^{-21}$, $p < 10^{-4}$, and $p < 10^{-6}$, for mouse 1, 2, and 3, respectively (binomial probability test).

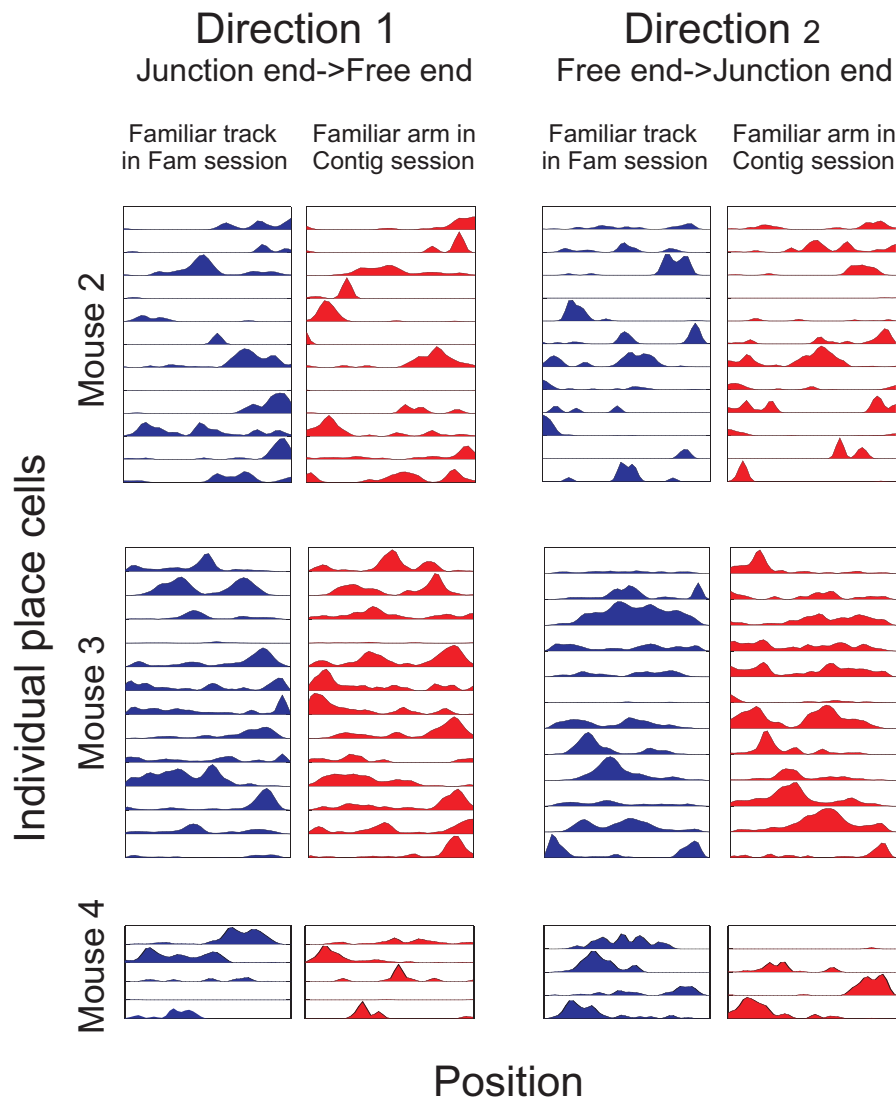


Figure S5 Stability of spatial tuning of place cells active on the familiar track across the novel experience. Comparison of spatial tuning of place cells active on the familiar track during the Fam session (blue) and Contig sessions (red) separated by direction of movement. Each row represents one cell active in the corresponding direction. For each cell, firing rates are on the same scale in the two run sessions. Note the relative stability of spatial tuning across novel experience. Data for Mice 2-4 are presented here, while data for Mouse 1 are presented in Fig. 1A, B. Statistical significance is presented in Fig. 2e.

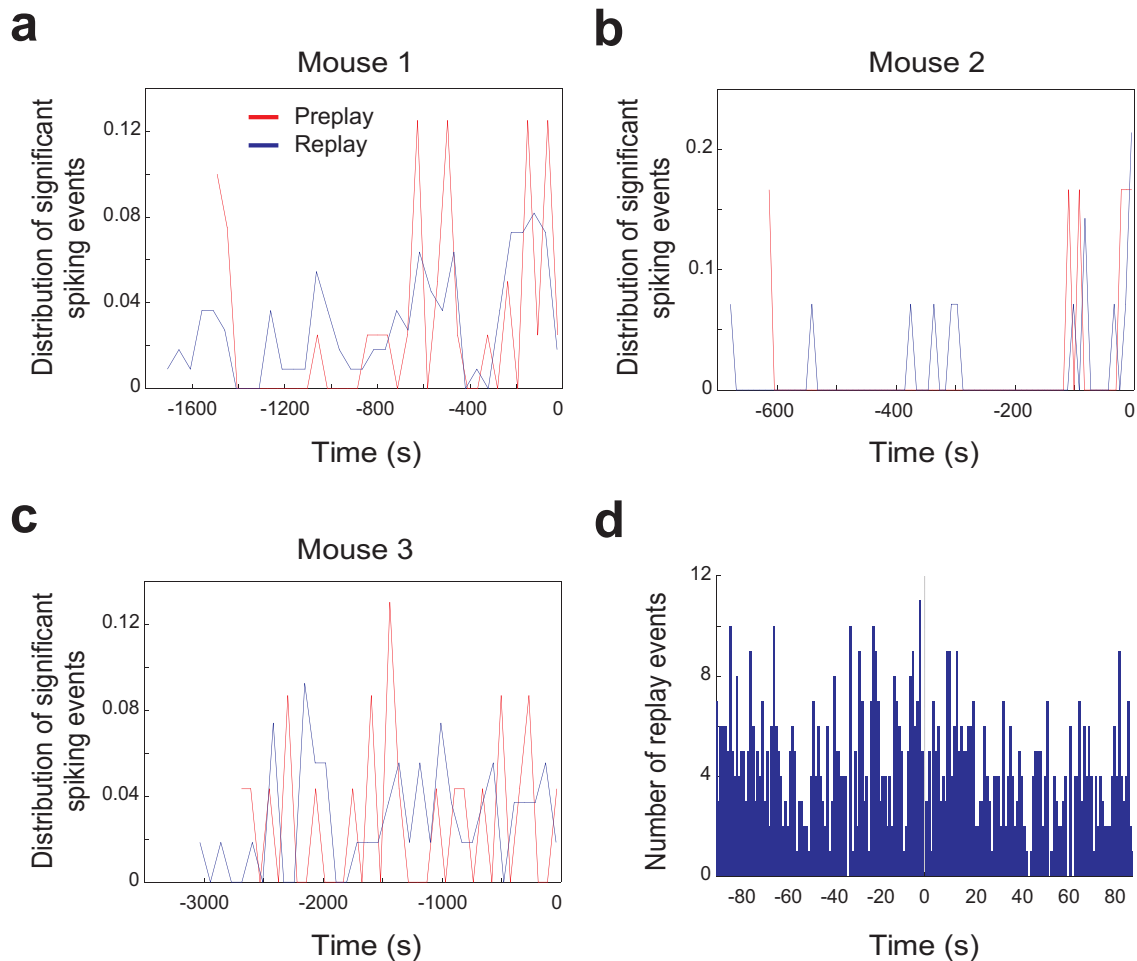


Figure S6 Distribution of preplay and replay events in time. **a-c**, Time distribution of preplay (red) and replay (blue) events of mice 1-3 during the Fam-Rest session. The negative values on the x-axis represent time before the opening of the barrier, which happened at time 0. The distributions were normalized by the total number of corresponding significant events for each mouse. **d**, Cross-correlation between the time of preplay (used as reference at 0 s) and the time of replay events. The spiking events that were significantly correlated with both the familiar track (replay) and the novel arm (preplay) were excluded from the analysis. The vertical dotted line marks the time of occurrence of preplay events.

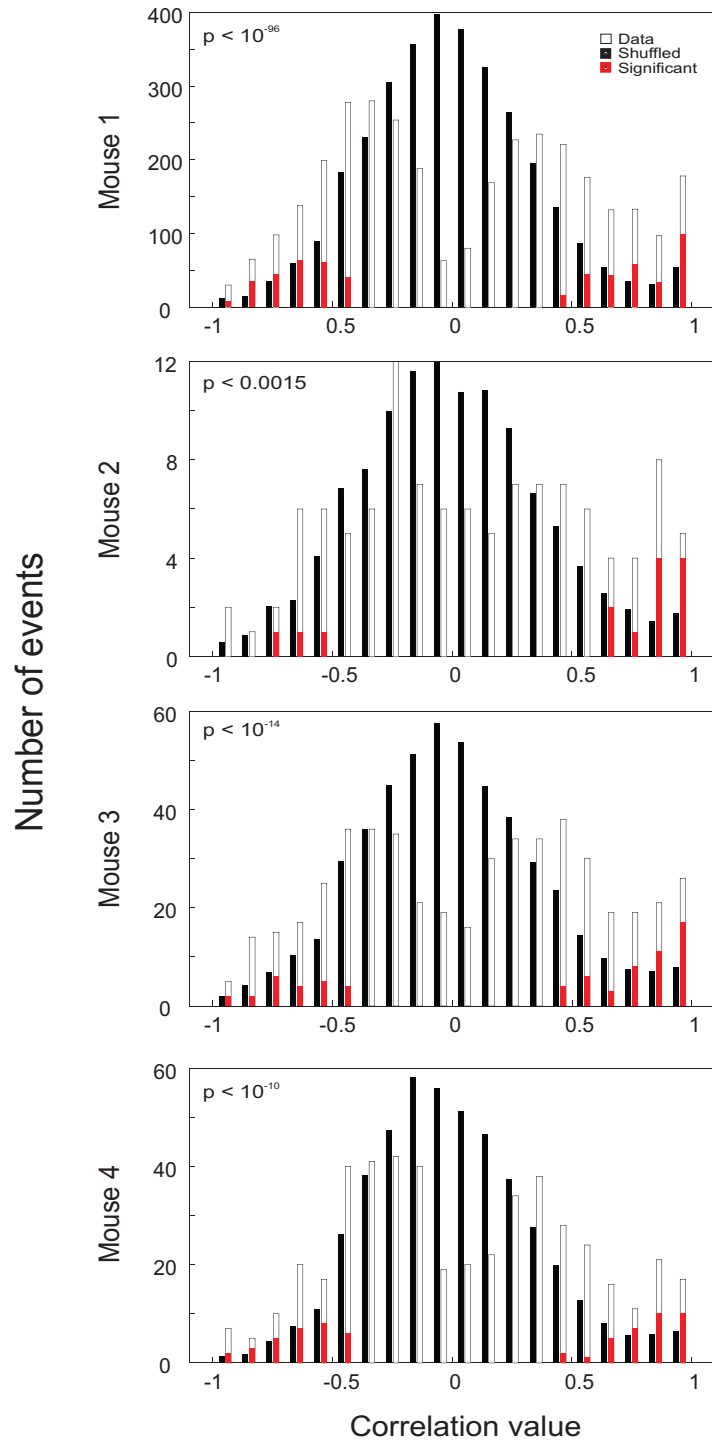


Figure S7 Quantification of the preplay phenomenon in individual mice in the De novo condition. Distribution of spiking events across rank-order correlation with the place cell sequence template of the novel track for all four individual animals. The top panel corresponds to examples shown in Fig. 4A

(Mouse 1). Open bars: spiking events vs. the original (unshuffled) template. Filled bars: spiking events vs. 200 shuffled templates. In order to obtain this distribution, the correlation value of each event vs. each randomly shuffled template was determined and the values from the 200 shuffled templates were scaled down 200 times. Red bars: distribution of significant preplay events (see the text for the definition of significance). P-values refer to results from the Kolmogorov-Smirnov test. The proportions of significant events out of the total number of spiking events were significant in each animal: $p < 10^{-100}$, $p < 10^{-6}$, $p < 10^{-30}$, and $p < 10^{-28}$, for mouse 1, 2, 3, and 4, respectively (binomial probability test).

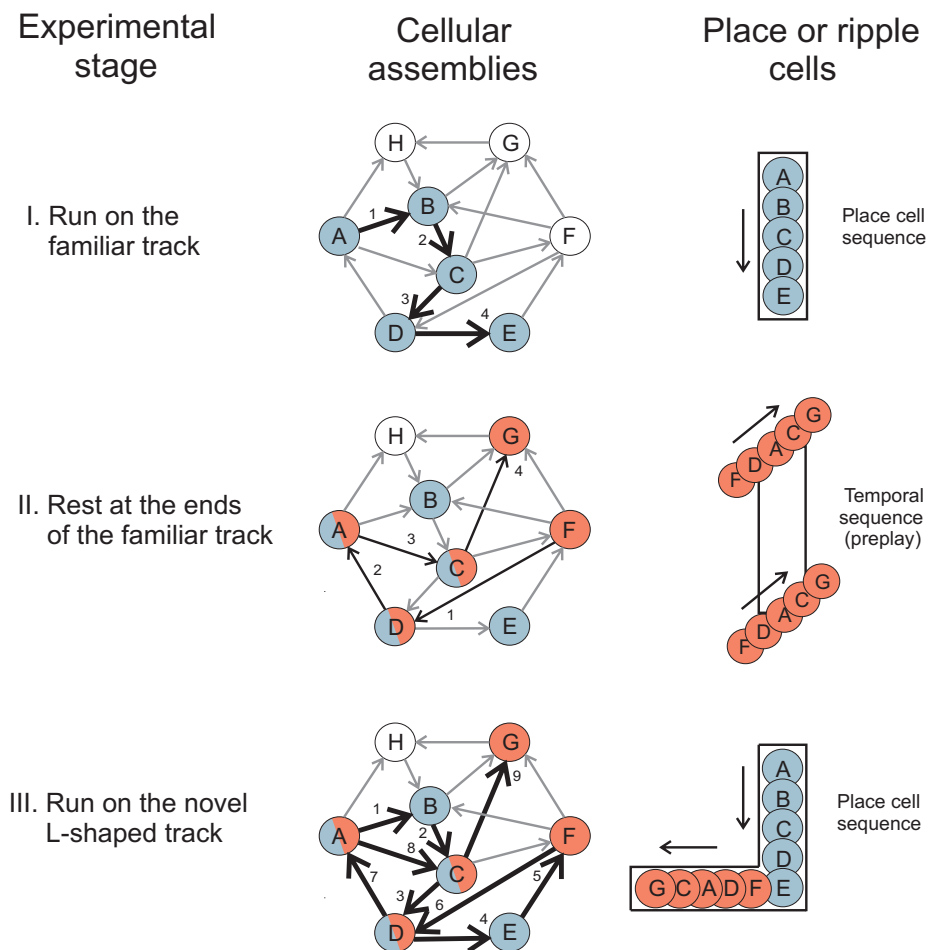


Figure S8 Cell-assembly model of preplay and temporal-to-spatial transformation in response to novel exploration. Left panels: network of

sequentially activated neurons during different experimental stages. Stage I, run on the familiar track; Stage II, rest at the ends of the familiar track; Stage III, run on the novel L-shaped track. Arrows indicate potential (thin) or actual (bold) temporal order of activation during Run in CA1, *not* anatomical connectivity. All thin arrows during Rest indicate the temporal order of activation during Rest. Black arrows during Rest emphasize temporal preplay. Upper case letters: corresponding individual cells/assemblies. Colours: sequential cell-assemblies co-active on a given linear track. Cells A, C, and D are active on both the familiar and novel tracks. White circles: cells with no place field during the corresponding run session. Right panels: sequences of place cells/assemblies on linear tracks under different conditions. Letters, colours, and order of activation correspond to the ones on the left. Arrows on the right represent the direction of the animal's movement (Run) or temporal preplay during ripples (Rest). This example illustrates a case of forward preplay. For reverse preplay, the order of activation of place cells on the track is opposite to their order of firing during preplay. During Rest (left), several possible sequences are activated (e.g., A>H; A>B>C>D>E; F>D>A>C>G; G->H, etc.), of which one (bold arrows) will result in a corresponding new sequence of place fields on the novel arm (right). Preplay occurs at the ends of tracks (stage II, right); the two examples do not necessarily occur in association with the same lap of running. Bold arrows during run also represent potentiated synaptic connectivity induced by the run experience upstream of CA1 (in CA3 or entorhinal cortex) while thin arrows represent non-potentiated existing synaptic connectivity upstream of CA1.